Multiscaling in Models of Magnetohydrodynamic Turbulence

Abhik Basu,[1] Anirban Sain,[1] Sujan K. Dhar,[2] and Rahul Pandit[1,*]
[1]*Department of Physics, Indian Institute of Science, Bangalore 560012, India*
[2]*Supercomputer Education and Research Center, Indian Institute of Science, Bangalore 560012, India*
(Received 15 October 1997)

From a numerical study of the magnetohydrodynamic (MHD) equations we show, for the first time in three dimensions ($d = 3$), that velocity and magnetic-field structure functions exhibit multiscaling, extended self-similarity (ESS), and generalized extended self-similarity (GESS). We propose a new shell model for homogeneous and isotropic MHD turbulence, which preserves all the invariants of ideal MHD, reduces to a well-known shell model for fluid turbulence for zero magnetic field, has no adjustable parameters apart from Reynolds numbers, and exhibits the same multiscaling, ESS, and GESS as the MHD equations. We also study the inertial- to dissipation-range crossover. [S0031-9007(98)07096-3]

PACS numbers: 47.27.Gs, 05.45.+b, 47.65.+a

The extension of Kolmogorov's work (K41) [1] on fluid turbulence to magnetohydrodynamic (MHD) turbulence yields [2] simple scaling for velocity $\mathbf{v}$ and magnetic-field $\mathbf{b}$ structure functions, for distances r in the *inertial range* between the forcing scale L and the dissipation scale η_d. Many studies have shown that there are multiscaling corrections to K41 in fluid turbulence [3]. Solar-wind data [4], numerical studies of two-dimensional MHD [5], and recent shell-model studies [6,7] of MHD turbulence yield similar multiscaling. We elucidate this for homogeneous, isotropic MHD turbulence, in the absence of a mean magnetic field, by presenting the first evidence for such multiscaling in a numerical, pseudospectral study of the MHD equations in *three dimensions* ($3d$MHD). We propose a shell model with no tunable parameters except Reynolds numbers, study it by an Adams-Bashforth method, show it has this multiscaling, and that it reduces to the Gledzer-Ohkitani-Yamada (GOY) shell model [8,9] for $3d$ fluid turbulence if $\mathbf{b} = \mathbf{0}$. To extract multiscaling exponents we develop the ideas of extended self-similarity (ESS) [10,11] and generalized extended self-similarity (GESS) [11,12] in both real and wave-vector (k) spaces, used in fluid turbulence [10–12].

We use the structure functions $S_p^a = \langle |a(\mathbf{x} + \mathbf{r}) - a(\mathbf{x})|^p \rangle$, where a can be $\mathbf{v}$, $\mathbf{b}$, or one of the Elsässer variables $\mathbf{Z}^{\pm} = \mathbf{v} \pm \mathbf{b}$, $\mathbf{x}$ and $\mathbf{r}$ are spatial coordinates, and the angular brackets denote an average in the statistical steady state. $S_p^a \sim r^{\zeta_p^a}$ at high fluid and magnetic Reynolds numbers Re and Re_b, respectively, and for the inertial range $20\eta_d \lesssim r \ll L$. The extension [2] of K41 to *homogeneous, isotropic* MHD turbulence *with no mean magnetic field* yields $\zeta_p^a = p/3$. Shell models [6,7] and solar-wind data [4] have obtained multiscaling in MHD turbulence, i.e., $\zeta_p^a = p/3 - \delta\zeta_p^a$, with $\delta\zeta_p^a > 0$ and ζ_p^a nonlinear, monotonically increasing functions of p. Work on fluid turbulence shows [3] an extended inertial range if we use ESS [10] and GESS [12]: Thus with ESS, in which ζ_p^a/ζ_3^a follows from $S_p^a \sim [S_3^a]^{\zeta_p^a/\zeta_3^a}$, we should expect by analogy that it extends down to $r \simeq 5\eta_d$ (as exploited in some MHD shell models [6,7]). In GESS, which employs $\mathcal{G}_p^a(r) \equiv S_p^a(r)/[S_3^a(r)]^{p/3}$ and postulates a form $\mathcal{G}_p^a(r) \sim [\mathcal{G}_q^a(r)]^{\rho_{pq}^a}$, with $\rho_{pq}^a = [\zeta_p^a - p\zeta_3^a/3]/[\zeta_q^a - q\zeta_3^a/3]$, it has been suggested [12] for fluid turbulence that the apparent inertial range is extended to the lowest resolvable r; however, k-space GESS [11] shows a crossover from inertial- to dissipation-range asymptotic behaviors.

Our studies yield many interesting results: The multiscaling exponents we obtain from 3DMHD and our shell model agree (Figs. 1a and 1b) and $\zeta_p^b > \zeta_p^{Z^+} \gtrsim \zeta_p^{Z^-} > \zeta_p^v$. ζ_p^b lie close to the She-Leveque (SL) prediction [13] for fluids ($\zeta_p^{\mathrm{SL}} = p/9 + 2[1 - (2/3)^{p/3}]$), but ζ_p^v lie below it (Fig. 1c) [14]. The probability distribution functions (Fig. 1d) for $\delta v_\alpha(\mathbf{r}) = v_\alpha(\mathbf{x} + \mathbf{r}) - v_\alpha(\mathbf{x})$ and $\delta b_\alpha(\mathbf{r}) = b_\alpha(\mathbf{x} + \mathbf{r}) - b_\alpha(\mathbf{x})$ are also different. ESS works both with real- and k-space structure functions (Fig. 2). To study the latter we postulate k-space ESS [for real-space structure functions we use $\mathcal{S}$ and $\mathcal{G}$ and for their k-space analogs (*not* Fourier transforms) S and G]:

$$
\begin{aligned}
S_p^a &\equiv \langle |a(\mathbf{k})|^p \rangle \approx A_{Ip}^a (S_3^a)^{\zeta_p'^a}, \qquad L^{-1} \ll k \lesssim 1.5k_d\,, \\
S_p^a &\equiv \langle |a(\mathbf{k})|^p \rangle \approx A_{Dp}^a (S_3^a)^{\alpha_p^a}, \qquad 1.5k_d \lesssim k \ll \Lambda\,,
\end{aligned}
\tag{1}
$$

where $a(\mathbf{k})$ is the Fourier transform of $a(\mathbf{r})$, A_{Ip}^a and A_{Dp}^a are, respectively, nonuniversal amplitudes for inertial and dissipation ranges, $k_d \sim \eta_d^{-1}$, and Λ^{-1} the (molecular) length at which hydrodynamics breaks down (cf. [11] for fluid turbulence). The exponents α_p^a and $\zeta_p'^a$ characterize the asymptotic behaviors of the structure functions in dissipation and inertial ranges. They are universal, but $\alpha_p^a \neq \zeta_p'^a$. In our shell model $\zeta_p'^a = \zeta_p^a$, but our data for 3DMHD suggest $\zeta_p'^a = 2(\zeta_p^a + 3p/2)/11$ (i.e., $S_p^a(k) \sim k^{-(\zeta_p^a + 3p/2)}$ in the inertial range [15]); the difference arises because of phase-space factors [11]. $\zeta_p'^a$ and α_p^a seem universal (the same for all our runs [Table I]); α_p^a is close to, but *systematically less* than, $p/3$. The k dependences

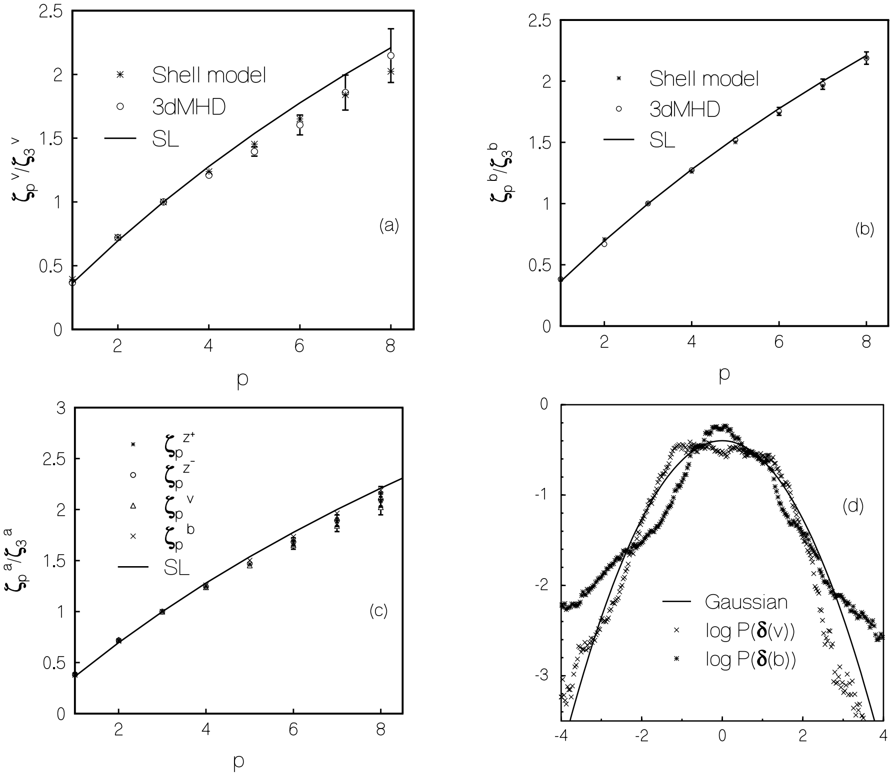

FIG. 1. (a)–(c) Inertial-range exponents versus p from typical 3DMHD and shell-model runs (Table I) and their comparison with the SL formula: (a) ζ_p^v/ζ_3^v, (b) ζ_p^b/ζ_3^b, and (c) ζ_p^v, ζ_p^b, $\zeta_p^{z^+}$, and $\zeta_p^{z^-}$ from SH2. (d) Semilog (base 10) plots of the probability distributions $P(\delta v_\alpha(r))$ and $P(\delta b_\alpha(r))$ with r in the dissipation range [we average over $6\tau_{ev}$ (Table I) and suppress α since we average over Cartesian components]; a Gaussian distribution is shown for comparison.

of S_p^a follow from that of S_3^a. We find

$$S_3^a \approx B_I^a k^{-\zeta_3^a - 9/2}, \qquad L^{-1} \ll k \lesssim 1.5 k_d\,, \qquad (2)$$

$$S_3^a \approx B_D^a k^{\delta^a} \exp(-c^a k/k_d), \qquad 1.5 k_d \lesssim k \ll \Lambda\,, \quad (3)$$

where B_I^a and B_D^a are nonuniversal amplitudes [Equation (2) holds [11] for 3DMHD; for our shell model the factor $9/2$ is absent]. Thus *all* $S_p^a \sim k^{\theta_p^a} \exp(-c^a \alpha_p^a k/k_d)$ for $1.5k_d \lesssim k \ll \Lambda$, with $\theta_p^a = \alpha_p^a \delta^a$ (cf. [11] for fluid turbulence). In Eq. (3) δ^a, c^a, and k_d are not universal; they depend on whether we use the 3DMHD equations or our shell model. We extract the *universal* part of the inertial- to dissipation-range crossover via our k-space GESS as follows: We first define $G_p^a \equiv S_p^a/(S_3^a)^{p/3}$; log-log plots of G_p^a versus G_q^a yield curves with *universal, but different,* slopes for asymptotes in inertial and dissipation ranges. The inertial-range asymptote has a slope $\rho_{p,q}^a$ (as in real-space GESS); the dissipation-range one has a slope $\omega^a(p,q) \equiv [\alpha_p^a - p/3]/[\alpha_q^a - q/3]$. These slopes are universal, but not the points at which the curves move away from the inertial-range asymptote. To obtain a *universal crossover scaling function* [different for each (p,q) pair because of multiscaling] we define $\log(H_{pq}^a) \equiv D_{pq}^a \log(G_p^a)$ and $\log(H_{qp}^a) \equiv D_{qp}^a \log(G_q^a)$; the scale factors $D_{pq}^a = D_{qp}^a$ are *nonuniversal,* but plots of $\log(H_{pq}^a)$ versus $\log(H_{qp}^a)$, for *both* 3DMHD and our shell model, collapse onto a *universal curve* within our error bars for *all* k, Re_λ, and $\mathrm{Re}_{b\lambda}$ (Fig. 3).

The MHD equations are [2]

$$\frac{\partial \mathbf{Z}^\pm}{\partial t} + (\mathbf{Z}^\mp \cdot \nabla)\mathbf{Z}^\pm = \nu_+ \nabla^2 \mathbf{Z}^\pm + \nu_- \nabla^2 \mathbf{Z}^\mp - \nabla p^* + \mathbf{f}^\pm, \qquad (4)$$

where $\nu_\pm \equiv (\nu_v \pm \nu_b)/2$, ν_v and ν_b are, respectively, fluid and magnetic viscosities, $p^* \equiv [p + (b^2/8\pi)]$,

TABLE I. The viscosities and hyperviscosities ν_v, ν_b, ν_{vH}, and υ_{bH}, the Taylor-microscale Reynolds numbers Re_λ and $\mathrm{Re}_{b\lambda}$, the box-size eddy-turnover times τ_{ev} and τ_{eb}, the averaging time τ_A, the time over which transients are allowed to decay τ_t, and k_d (dissipation-scale wave number) for our 3DMHD runs ($k_{\max} = 32$ for MHD1 and MHD2 and $k_{\max} = 40$ for MHD3) and shell-model runs SH1–4 ($k_{\max} = 2^{25} k_0$). The step size (δt) is 0.02 for MHD1–3, 2×10^{-5} for SH1–2, and 10^{-4} for SH3–4. Note that $\tau_{ev} \simeq 8\tau_I$ the integral time for our 3DMHD runs.

Run	ν_v	ν_{vH}	ν_b	ν_{bH}	Re_λ	$\mathrm{Re}_{m\lambda}$	$\tau_{ev}/\delta t$	$\tau_{ev}/\delta t$	τ_t/τ_{ev}	τ_A/τ_{ev}	$k_{\max}/k_d$
MHD1	8×10^{-4}	7×10^{-6}	10^{-3}	8×10^{-6}	$\simeq 24.8$	$\simeq 14.3$	$\simeq 8.8 \times 10^3$	$\simeq 6 \times 10^3$	$\simeq 2$	$\simeq 2.3$	$\simeq 1.83$
MHD2	8×10^{-4}	9×10^{-6}	8×10^{-4}	9×10^{-6}	$\simeq 24.1$	$\simeq 18.1$	$\simeq 8.8 \times 10^3$	$\simeq 5.6 \times 10^3$	$\simeq 2$	$\simeq 2.3$	$\simeq 1.83$
MHD3	8×10^{-4}	9×10^{-6}	8×10^{-4}	9×10^{-6}	$\simeq 26$	$\simeq 19.6$	$\simeq 7.9 \times 10^3$	$\simeq 4.8 \times 10^3$	$\simeq 1$	$\simeq 2.2$	$\simeq 2.22$
SH1	10^{-9}	0	10^{-9}	0	$\simeq 4.6 \times 10^8$	$\simeq 7.8 \times 10^8$	$\simeq 10^7$	$\simeq 6 \times 10^6$	$\simeq 50$	$\simeq 450$	$\simeq 2^5$
SH2	10^{-8}	0	10^{-8}	0	$\simeq 4.3 \times 10^7$	$\simeq 6.5 \times 10^7$	$\simeq 10^7$	$\simeq 6 \times 10^6$	$\simeq 50$	$\simeq 450$	$\simeq 2^8$
SH3	10^{-6}	0	2×10^{-6}	0	$\simeq 4 \times 10^6$	$\simeq 3 \times 10^6$	$\simeq 2 \times 10^6$	$\simeq 10^6$	$\simeq 500$	$\simeq 2500$	$\simeq 2^{10}$
SH4	4×10^{-6}	0	10^{-6}	0	$\simeq 1.2 \times 10^5$	$\simeq 1 \times 10^6$	$\simeq 10^6$	$\simeq 1.7 \times 10^6$	$\simeq 500$	$\simeq 3000$	$\simeq 2^{11}$

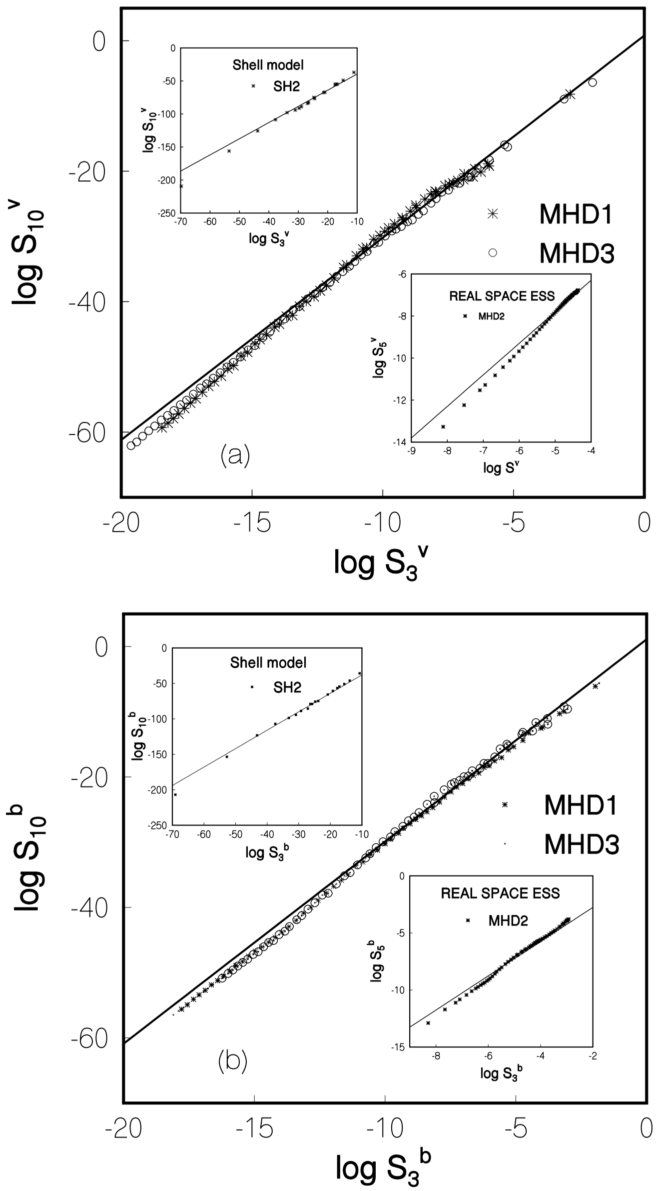

FIG. 2. Log-log plots (base 10) of S_{10}^a versus S_3^a showing k space ESS for 3DMHD with (a) $a = \mathbf{v}$ and (b) $a = \mathbf{b}$. Insets illustrate real-space ESS for 3DMHD and ESS for our shell model; the lines show the inertial-range asymptotes (a few points on the right correspond to forcing scales and are not used for inertial-range fitting).

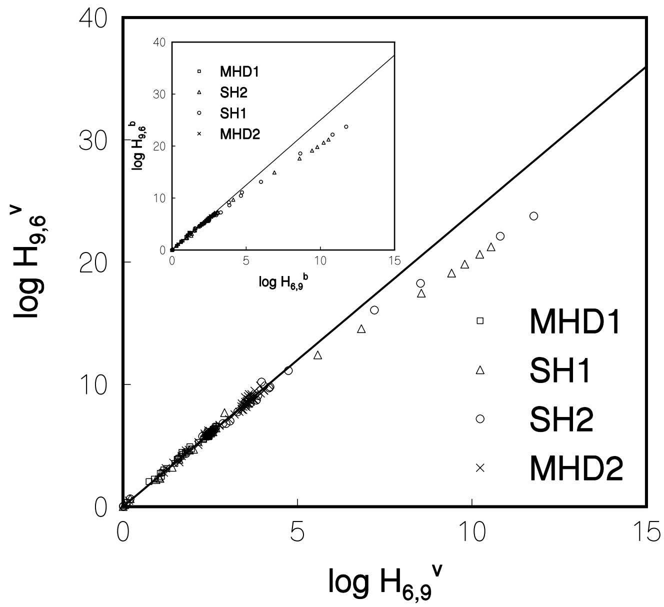

FIG. 3. GESS log-log plots (base 10) of $H_{9,6}^v$ versus $H_{6,9}^v$ and (inset) $H_{9,6}^b$ versus $H_{6,9}^b$ showing the inertial- to dissipation-range crossover; lines are inertial-range asymptotes.

with p the pressure, the density $\rho = 1$, $\mathbf{f}^{\pm} \equiv (\mathbf{f} \pm \mathbf{g})/2$, and $\mathbf{f}$ and $\mathbf{g}$ are the forcing terms in the equations for $\partial \mathbf{v}/\partial t$ and $\partial \mathbf{b}/\partial t$. We assume incompressibility and use a pseudospectral method [11] to solve Eq. (4) numerically. We force the first two k shells, use a cubical box with side $L_B = 2\pi$, periodic boundary conditions, and 64^3 modes in runs MHD1 and MHD2 and 80^3 modes in run MHD3 (Table I). We include fluid and magnetic hyperviscosities ν_{vH} and ν_{bH} [i.e., the term $-(\nu_v + \nu_{vH} k^2) k^2$ in the equation for $\partial \mathbf{v}(\mathbf{k})/\partial t$ and the term $-(\nu_b + \nu_{bH} k^2) k^2$ in the equation for $\partial \mathbf{b}(\mathbf{k})/\partial t$] [16]. For time integration we use an Adams-Bashforth scheme (step-size δt). We use $\mathrm{Re}_\lambda = v_{\mathrm{rms}} \lambda/\nu_v$, $\mathrm{Re}_{b\lambda} = b_{\mathrm{rms}} \lambda/\nu_b$, $\lambda_v = [\int_o^\infty E_v(k)\, dk / \int_o^\infty k^2 E_v(k)\, dk]^{1/2}$, $\lambda_b = [\int_o^\infty E_b(k)\, dk / \int_o^\infty k^2 E_b(k)\, dk]^{1/2}$, $E_v(k) \sim S_2^v(k) k^2$, and $E_b(k) \sim S_2^b(k) k^2$. Parameters for runs MHD1–3 are given in Table I, where $\tau_{ea} \equiv L_B/a_{\mathrm{rms}}$ is the box-size eddy-turnover time for field a and τ_A the averaging time; initial transients are allowed to decay over a period τ_t. We use quadruple-precision arithmetic; results from our 64^3 and 80^3 runs are not significantly different.

The Richardson-cascade picture suggests that the multiscaling behavior in turbulence might arise in simplified dynamical models with a reduced number degrees of freedom arranged hierarchically. Shell models of turbulence [3,8], which cannot be derived from the Navier-Stokes equation, but build in the cascade and all conservation laws, achieve this reduction with complex scalar velocities in a logarithmically discretized k space; they obtain large Re_λ and exponents in agreement with experiments. Similar shell models for MHD turbulence have been proposed earlier [6,7,17], but there is *no* MHD shell model that enforces *all* ideal 3DMHD invariants *and* which reduces to the GOY shell model for fluid turbulence, when magnetic-field terms are suppressed. We present such a model and show that it yields ζ_p^a in agreement with those we obtain for 3DMHD. Our shell-model equations

$$\frac{dz_n^{\pm}}{dt} = i c_n^{\pm} - \nu_+ k_n^2 z_n^{\pm} - \nu_- k_n^2 z_n^{\mp} + f_n^{\pm} \qquad (5)$$

use the *complex, scalar* Elsässar variables $z_n^{\pm} \equiv (v_n \pm b_n)$, and discrete wave vectors $k_n = k_o q^n$, for shells n; $c_n^{\pm} = [a_1 k_n z_{n+1}^{\mp} z_{n+2}^{\pm} + a_2 k_n z_{n+1}^{\pm} z_{n+2}^{\mp} + a_3 k_{n-1} z_{n-1}^{\mp} z_{n+1}^{\pm} + a_4 k_{n-1} z_{n-1}^{\pm} z_{n+1}^{\mp} + a_5 k_{n-2} z_{n-1}^{\mp} z_{n-2}^{\pm} + a_6 k_{n-2} z_{n-1}^{\pm} z_{n-2}^{\mp}]^*$, which ensures $z_n^+,\ z_n^- \sim k^{-1/3}$ is a stationary solution in the inviscid, unforced limit

[6–9] and preserves the $\nu_+, Z^+ \leftrightarrow \nu_-, Z^-$ symmetry of 3DMHD. We fix five of the parameters, $a_1 - a_6$, by demanding that our shell-model analogs of the total energy $[\equiv \sum_n(|v_n|^2 + |b_n|^2)/2]$, the cross helicity $[\equiv 1/2 \sum_n (v_n b_n^* + v_n^* b_n)]$, and the magnetic helicity $[\equiv \sum_n (-1)^n |b_n|^2/k_n]$ be conserved if $\nu_\pm = 0$ and $f_n^\pm = 0$; while enforcing the conservation of energy, we also demand [18] that the cancellation of terms occurs as in 3DMHD. We fix the last parameter by demanding that, if $b_n = 0$ for all n, our model reduces to the GOY model, with the standard parameters [9] that enforce conservation laws. Finally $a_1 = 7/12$, $a_2 = 5/12$, $a_3 = -1/12$, $a_4 = -5/12$, $a_5 = -7/12$, $a_6 = 1/12$, and $q = 2$. We solve Eq. (5) numerically by an Adams-Bashforth scheme (step size δt), use 25 shells, force the first k shell [11], set $k_o = 2^{-4} = 1/(2L_s)$, where L_s is the box size, and use $E_v = S_2^v(k_n)/k_n$, $\lambda_v = (2\pi/k_o)[\sum_n S_2^v(k_n)/\sum_n k_n^2 S_2^v(k_n)]^{1/2}$, $\lambda_b = (2\pi/k_o)[\sum_n S_2^b(k_n)/\sum_n k_n^2 S_2^b(k_n)]^{1/2}$, $v_{\mathrm{rms}} = [k_o \sum_n S_2^v(k_n)/\pi]^{1/2}$, and $b_{\mathrm{rms}} = [k_o \sum_n S_2^b(k_n)/\pi]^{1/2}$. Parameters for our four runs SH1–SH4 are given in Table I. These use double-precision arithmetic, but we have checked in representative cases that our results are not affected if we use quadruple-precision arithmetic. As in the GOY model the structure functions $S_p(k_n)$ oscillate weakly with k_n because of an underlying three cycle [9,18]. These oscillations can be removed either (a) by using ESS or (b) by using the structure functions $\sum_{n,p}^a = \langle \mathrm{Im}[a_n a_{n+1} a_{n+2} + a_{n-1} a_n a_{n+1}/4]^{p/3} \rangle$ [9]. Method (a) yields ζ_p^a/ζ_3^a, which we find are universal. Method (b) gives exponents ζ_p^a. These have a mild dependence on Re_λ and $\mathrm{Re}_{b\lambda}$ but this goes away if we consider the ratios ζ_p^a/ζ_3^a, as in the GOY model [11]; thus the asymptotes in our ESS and GESS plots have universal slopes.

The Navier Stokes equation (3DNS) follows from 3DMHD if $\mathbf{b} = \mathbf{0}$ or, equivalently, $\mathrm{Re}_{b\lambda} = 0$. However, if we start with $\mathrm{Re}_{b\lambda} \simeq 0$, the steady state is characterized by the MHD exponents and $\mathrm{Re}_\lambda/\mathrm{Re}_{b\lambda} \simeq O(1)$ (i.e., an equipartition regime) [19]. Since our MHD shell model reduces to the GOY model as $\mathrm{Re}_{b\lambda} \to 0$, we use it (and not costly 3DMHD) to study the fluid turbulence to MHD turbulence crossover: A small initial value of $\mathrm{Re}_{b\lambda}$ yields a transient with GOY-model exponents, but finally the system crosses over to the MHD turbulence steady state [18].

In summary, we have shown that structure functions in 3DMHD turbulence display multiscaling, ESS, and GESS, with exponents and probability distributions different from those in fluid turbulence. Our new shell model (a) gives the same exponents as 3DMHD and (b) reduces to the GOY model as $\mathrm{Re}_{b\lambda} \to 0$. Our ESS and GESS uncover a universal crossover from inertial- to dissipation-range asymptotics. It would be interesting to compare our results with experiments, but with caution: (i) solar-wind data might yield exponents different from ours because of the presence of a mean magnetic field and compressive effects [20]; (ii) the inertial- to dissipation-range crossover might not apply to the solar wind because a hydrodynamic description might break down in the dissipation range [20]. However, our results should apply to MHD systems with an equipartition regime [2]. The agreement of ζ_p^b with the SL formula is interesting but, we believe, fortuitous since vorticity organizes itself into filamentary structures [13] in fluid turbulence but into sheetlike structures in 3DMHD (we have checked this in our study).

We thank J. K. Bhattacharjee and S. Ramaswamy for discussions, CSIR (India) for support, and SERC (IISc, Bangalore) for computational resources.

*Also at Jawaharlal Nehru Centre for Advanced Scientific Research, Bangalore, India.

[1] A. N. Kolmogorov, C. R. Acad. Sci. USSR **30**, 301 (1941).
[2] D. Montgomery, in *Lecture Notes on Turbulence*, edited by J. R. Herring and J. C. McWilliam (World Scientific, Singapore, 1989); D. Biskamp, in *Nonlinear Magnetohydrodynamics*, edited by W. Grossman *et al.* (Cambridge University Press, Cambridge, England, 1993).
[3] For recent reviews, see K. R. Sreenivasan and R. A. Antonia, Annu. Rev. Fluid Mech. **29**, 435 (1997); S. K. Dhar *et al.*, Pramana J. Phys. **48**, 325 (1997).
[4] R. Grauer, J. Krug, and C. Marliani, Phys. Lett. **195**, 335 (1994); L. F. Burlaga, J. Geophys. Res. **96**, 5847 (1991); Horbury *et al.*, Adv. Space Res. **19**, 847 (1996).
[5] R. Grauer *et al.*, Phys. Plasmas **2**, 41 (1995).
[6] D. Biskamp, Phys. Rev. E **50**, 2702 (1994) also finds $\zeta_p^b > \zeta_p^v$, for $p = 2$, in a shell model.
[7] V. Carbone, Phys. Rev. E **50**, R671 (1994).
[8] E. B. Gledzer, Sov. Phys. Dokl. **18**, 216 (1973); K. Ohkitani and M. Yamada, Prog. Theor. Phys. **81**, 329 (1989).
[9] L. Kadanoff, D. Lohse, and J. Wang, Phys. Fluids **7**, 517 (1995).
[10] R. Benzi *et al.*, Phys. Rev. E **48**, R29 (1993).
[11] S. K. Dhar, A. Sain, and R. Pandit, Phys. Rev. Lett. **78**, 2964 (1997).
[12] R. Benzi *et al.*, Europhys. Lett. **32**, 709 (1995); for GESS in solar-wind data V. Carbone, Geophys. Res. Lett. **23**, 121 (1996); R. Grauer, Phys. Plasmas **2**, 41 (1995).
[13] Z. S. She and E. Leveque, Phys. Rev. Lett. **72**, 336 (1994).
[14] We use the SL formula as a convenient parametrization for the multiscaling exponents in fluid turbulence.
[15] For a heuristic justification for fluid turbulence, see [11].
[16] Hyperviscosities do not influence multiscaling (Ref. [11] for fluids) in the inertial range, where conventional viscosities dominate. Even if the viscosity vanishes, hyperviscosity does not affect ζ_p/ζ_3 in fluid turbulence [E. Leveque and Z. S. She, Phys. Rev. Lett. **75**, 2690 (1995)].
[17] C. Gloaguen *et al.*, Physica (Amsterdam) **17D**, 154 (1985).
[18] A. Basu and R. Pandit (unpublished).
[19] Thus in a renormalization-group calculation $\mathrm{Re}_{b\lambda}$ should appear as a relevant operator.
[20] E. Marsch, in *Reviews in Modern Astronomy Vol. 4*, edited by G. Klare (Springer-Verlag, Berlin, 1991); C.-Y. Tu and E. Marsch, Space Sci. Rev. **73**, 1 (1995).